Fabrication of nano-capillary emitter arrays for ionic liquid electrospray thrusters

Kanta Suzuki[1,2], Masayoshi Nagao[2], Yongxun Liu[2], Katsuhisa Murakami[2], Sommawan Khumpuang[2,3], Shiro Hara[2,3], and Yoshinori Takao[4*]

[1]*Department of Mechanical Engineering, Materials Science, and Ocean Engineering, Yokohama National University, Yokohama, 240-8501, Japan*

[2]*Device Technology Research Institute, National Institute of Advanced Industrial Science and Technology, Tsukuba, 305-8568, Japan*

[3]*Minimal Fab Promoting Organization, Tsukuba, 305-8568, Japan*

[4]*Division of Systems Research, Yokohama National University, Yokohama, 240-8501, Japan*

[*]E-mail: takao@ynu.ac.jp

Abstract

In this study, we fabricated nano-capillary emitter arrays for stable ion emission of ionic liquid electrospray thrusters, employing the fabrication of field emitter arrays or gated nano electron sources. A nano-capillary emitter was successfully fabricated with a 100–300-nm capillary diameter, which prevented ionic liquid leakage by significantly increasing the fluidic impedance of the ionic liquid compared to a previously proposed emitter. An ion emission experiment was conducted with 1-ethyl-3-methylimidazolium dicyanamide as the propellant.

Ion emission started at a low voltage of 61 V owing to a small gap of approximately 1 μm between the emitter and extractor electrode. The maximum current density was 43 mA cm^{-2} on the positive side and −13 mA cm^{-2} on the negative side without leakage of the ionic liquid, which was more than 100 times higher than that of conventional electrospray thrusters. Moreover, we obtained continuous ion emission without current intercepted by the extractor.

1. Introduction

As nanosatellites (1–10 kg) can be developed at low cost and in a short period of time, several hundreds of them are launched per year.[1)] Recently, a wide variety of uses for satellites have been proposed, including advanced missions, such as communication and earth observation by a satellite constellation and deep space exploration. These missions require thrusters for active orbit control to perform formation flight and orbit transition.[2,3)] However, thrusters mounted on nanosatellites are subject to strict size restrictions. Although ion thrusters have been mounted on a 50-kg-class microsatellite and successfully operated in space,[4)] it is difficult to mount them on nanosatellites due to their massive and bulky gas supply system. The entire propulsion system mounted on nanosatellites should fit within a cube approximately 10 cm on a side; thus, the area of the thruster head is also restricted to approximately several centimeters in diameter. Electrospray thrusters using ionic liquid as the propellant can be easily miniaturized because they do not require a gas supply system; therefore, many studies have recently been conducted on this topic.[5–10)]

Figure 1 presents a schematic of the ion source of an ionic liquid electrospray thruster. The ion source mainly consists of an emitter array and an extractor. The emitter array contains multiple capillaries with sharp tips from which ions are emitted. When a voltage is applied between the emitter and extractor, the electric field is concentrated at the emitter tip, which deforms the ionic liquid. Ion emission starts as the force of the field overcomes the back

pressure caused by the surface tension of the liquid. The emitted ions are accelerated downstream to produce thrust. The ionic liquid consists of only positive and negative ions without solvent.[11] Due to the Coulomb force between the ions, the vapor pressure of the ionic liquid is negligible. Therefore, the ionic liquid can exist in the liquid phase even in vacuum, simplifying the propellant feed system and reducing the size of the entire propulsion system.

However, the thrust produced by electrospray thrusters per emitter is too small, and the thrust density (~10 μN cm^{-2}) is less than one-tenth that of ion thrusters (> 100 μN cm^{-2}).[12] Increasing the emitter density is a possible method for improving the thrust density. In previous work, we proposed a high-density emitter array employing the fabrication of field emitter arrays (FEAs) or gated nano electron sources.[13,14] An emitter density of 4 million emitters cm^{-2} was achieved, which was approximately 10,000 times higher than that of conventional electrospray thrusters.[5–10] In a previous study, Spindt reported field-ionization sources for mass spectrometry employing the FEA process, which ionized the analyte gas by applying a high voltage of the order of 1 kV to the emitters.[15] In our previous work, the ion sources emitted ions from an ionic liquid, not gas, and the driving voltage was less than 100 V.[13]

In an ion emission experiment with the high-density emitter array fabricated in our previous study, the maximum current density was −1.4 mA cm^{-2} and 0.85 mA cm^{-2} for the negative and positive ion currents, respectively.[13] These values were approximately three times higher than the current density achieved by conventional electrospray thrusters;[5] however, they were still insufficient in consideration of the increase in emitter density. After investigation, we

detected leakage of the ionic liquid to the outside of the extractor, which inhibited stable ion emission. To solve the leakage problem, it may be effective to increase the fluidic impedance by an extremely narrow flow path of the ionic liquid.

In this paper, we fabricated an emitter array with a nano-sized emitter capillary that can be 100–300 nm in diameter and greatly increases the fluidic impedance. After fabrication, an ion emission experiment was conducted to evaluate the effect of the narrower flow path of the ionic liquid. The purpose of this study is to present a fabrication method for nano-capillary emitter arrays employing the fabrication of FEAs and to demonstrate stable ion emission by the nano-sized emitter capillary. In Sect. 2, we present the design of the nano-capillary emitter array and describe its fabrication procedure. In Sect. 3, we present the results of ion emission experiments with the fabricated arrays, where the arrays produced a current density 100 times higher than that of conventional electrospray thrusters. Conclusions are presented in Sect. 4.

2. Fabrication of nano-capillary emitter array

2.1. Nano-capillary emitter design

Figure 2 presents a schematic of an electrospray thruster for high thrust density, consisting of a nano-capillary emitter array, an extractor, and accelerator electrodes. In the nano-capillary emitter array, the emitter pitch can be 5 μm, which signifies that the emitter density can be 4 million emitters cm^{-2}. The inner diameter of the tip of the capillary emitter can be less than 100 nm, as illustrated in Fig. 2, whereas the inner diameter of the previously fabricated capillary

emitters is approximately 700 nm.[13] The extractor is formed on a 1-μm-thick insulating layer, signifying that the distance between the emitter and extractor is 1 μm, and its aperture is self-aligned to each emitter. This small gap between the emitter and extractor enables lower-voltage operation for ion emission, which implies that the emitter array can be used as an ultra-low energy ion beam source.[16] However, low-voltage operation is not desirable for propulsion applications from the viewpoint of the thrust T and specific impulse I_{sp}, defined as[17]

$$T = \sqrt{\frac{2M}{q}} I_{\mathrm{b}} \sqrt{V_{\mathrm{b}}}, \tag{1}$$

$$I_{\mathrm{sp}} = \frac{T}{\dot{m} g_0}, \tag{2}$$

respectively, where M is the ion mass, q is the ion charge, I_{b} is the ion beam current, V_{b} is the net voltage through which the ion is accelerated, $\dot{m}$ is the propellant mass flow rate, and g_0 is the acceleration of gravity.

Conventional electrospray thrusters are operated at a high voltage of several kV to obtain high thrust and specific impulse. However, our device cannot be operated at such a high voltage due to breakdown between the emitter and extractor. Therefore, an accelerator electrode can be added to enable high-voltage operation in future work. In our device, ionic liquid is supplied from the back side of the array. It is known that an emitter electrode composed of metal undergoes an electrochemical reaction with the ionic liquid, which leads to erosion of the emitter.[18,19] To overcome this problem, it is effective to fabricate the emitter with an insulating material and apply a voltage to the ionic liquid through a distal electrode located upstream of the emitter.[19] In our fabrication, we used silicon nitride (SiN) as the emitter material, and the

distal electrode was fabricated on the back side of the emitter array, as illustrated in Fig. 2.

The nano-capillary emitter has an extremely narrow flow path of the ionic liquid, which effectively increases the fluidic impedance. Fluidic impedance is associated with liquid transportation,[20] and high impedance inhibits the increase in the flow rate of the ionic liquid.[21] The impedance of the capillary under the assumption of Hagen–Poiseuille flow is expressed as

$$\frac{128\mu L}{\pi D^4}, \tag{3}$$

where μ is the fluid viscosity, L is the capillary length, and D is the capillary diameter, illustrated in Fig. 1. Because the capillary diameter of the nano-capillary emitter is a fraction of that of the previous emitter,[13] high fluidic impedance can be achieved, as it is inversely proportional to D^4.

The wettability of the capillary emitter is also an essential factor. The low wettability of the emitter causes the ionic liquid to remain at the tip of the emitter because the edge of the emitter tip prevents the liquid from wetting and spreading over the emitter surface. We controlled the wettability of SiN by CHF_3 plasma treatment. CHF_3 plasma is commonly used for etching SiO_2 in the reactive ion etching (RIE) process and is known to form a fluorocarbon layer on the material surface.[22] The fluorocarbon layer is expected to reduce the wettability of SiN. Figure 3 presents images of the ionic liquid on a CHF_3-treated SiN film and untreated SiN film. We used the ionic liquid of 1-ethyl-3-methylimidazolium dicyanamide (EMI-DCA), which is often used for electrospray thrusters because ions tend to be emitted in the ion mode instead of the droplet mode.[23] After 1.5 μL of EMI-DCA was dropped on each material, the

contact angle was calculated by the half-angle method. As illustrated in Fig. 3, the contact angles of EMI-DCA were 87.2° and 37.5° for the CHF_3-treated SiN film and untreated SiN film, respectively. This result indicates that CHF_3-treated SiN has lower wettability than untreated SiN. Thus, we used CHF_3-treated SiN as the emitter material.

2.2. Fabrication process of nano-capillary emitter array

Figure 4 presents the fabrication process of the nano-capillary emitter array. First, an Al layer (100 nm) was deposited by sputtering on a Si wafer, which served to stop the deep reactive ion etching (deep-RIE) process later. Thereafter, Ni conical emitters were formed on the Al layer using the fabrication of a volcano-structured double-gate Spindt-type FEA, as illustrated in Fig. 4(a).[14,24,25] A thin SiN layer (50 nm) was deposited over the emitters and etched at the tip of the emitters by the etch-back method, as illustrated in Fig. 4(b).[26] Although a photolithography process with 0.5 μm resolution is required for Ni conical emitter formation, an emitter capillary diameter of less than 100 nm can be formed without a photolithography process using the processes in Figs. 4(a) and (b). A SiO_2 layer (1 μm) was then deposited by plasma-enhanced chemical vapor deposition as an insulator between the electrodes. The extractor was also formed by the etch-back method for the sputtered Nb layer (200 nm) on SiO_2, as illustrated in Fig. 4(c). The emitter tip was uncovered by removing the SiO_2 insulating layer at the tip by buffered HF wet etching, as illustrated in Fig. 4(d). After the Cr mask (200 nm) was formed on the back side of the wafer, the ionic liquid reservoir was fabricated by the deep-RIE process from the back

side, as illustrated in Fig. 4(e). Finally, the ionic liquid flow path was formed by removing the Al etch-stop layer and the Ni Spindt-type emitters with a wet etching process, as illustrated in Fig. 4(f). It should be noted that the SiN layer was directly formed over the Ni cones to fabricate the nano-capillary emitter, whereas in the previous fabrication process, a SiO_2 insulating layer was also deposited on the Ni cones before the emitter electrode.[13] This direct emitter fabrication shortened the entire SiO_2 fabrication process of the Ni emitters. Moreover, in this fabrication, we used a minimal fab system for all photolithography processes and the deep-RIE process for the ionic liquid reservoir, as illustrated in Fig. 4(e).[27,28] This system is suitable for multi-product and low-volume manufacturing, such as for spacecraft devices.

Figure 5 presents scanning electron microscopy (SEM) images of the emitter array and one emitter and extractor set. The emitter density reached 4 million emitters cm^{-2} by fabrication with a 5-μm emitter pitch. As illustrated in Fig. 5, the Ni cones were successfully removed, and the nano-capillary emitter was fabricated. The inset of Fig. 5(b) presents the top-view image of the nano-capillary emitter, where a 108-nm capillary diameter of the emitter was achieved. SEM imaging demonstrated that the diameter of the emitter capillary formed by the etch-back method varied depending on the emitter position in a wafer and the etch-back time of each wafer. When the capillary diameters of 80 emitters in one wafer (Wafer A) were measured, the average diameter was 258 nm with a standard deviation of 38 nm. Thereafter, we reduced the etch-back time in another wafer (Wafer B) and measured the diameter of 65 emitters. The results revealed that the average diameter was 167 nm with a standard deviation of 47 nm.

The diameter variation is caused by differences in the Ni cone height, resist thickness, and resist etching rate in the etch-back process. Of these factors, the difference in Ni cone height has a dominant effect on the diameter variation because the variations of the resist thickness and etching rate are negligible. Therefore, by obtaining a uniform Ni conical emitter array, we can achieve the desired capillary diameters within the range of the Ni cone's tip curvature and base diameter by precisely adjusting the etch-back time.

3. Ion emission experiment

Figure 6 presents the experimental setup for the measurement of the ion emission current. The measurement was performed in a vacuum chamber at a pressure of less than 1.0×10^{-3} Pa. We prepared nano-capillary emitter arrays within a 300-μm diameter area that had a different number of emitters: 10 × 10, 20 × 20, 40 × 40, and 2,593 (maximum number of emitters with 5-μm pitch in a 300-μm diameter circle). These arrays were integrated within a half-inch wafer as an independent emission area. Then, 0.1 μL of EMI-DCA was dropped on the back side of the emitter array with a micropipette. Here, the flow rate of the ionic liquid was not actively controlled. The ionic liquid was connected to a source meter (Keithley 2636A) through a 1-MΩ resistor via the distal electrode on the back side of the array. A bipolar pulse voltage of 5 Hz was applied to the extractor by the source meter (Keithley 2636A) through a 100-kΩ resistor. The collector electrode for measuring the ion emission current was placed 1 mm downstream of the emitter array. A 5-Hz bipolar pulse was also applied to the collector by another source

meter (Keithley 2657A), where the amplitude was fixed at 500 V and the polarity was always the same as that of the extractor voltage.

It should be noted that the potential structure was opposite that illustrated in Figs. 1 and 2. In the electrospray thruster concept, the outermost electrode (extractor in Fig. 1 and accelerator electrode in Fig. 2) is connected to the ground potential to accelerate ions to the outside of the spacecraft. In contrast, in the present study, the distal electrode was grounded, and bipolar pulse voltage was applied to the extractor. The reason for this was that the distal electrode was common to all emission areas of the wafer, and we needed to apply voltage to each emission area to investigate the emission characteristics independently. Since the collector electrode was always more strongly biased than the extractor, the present potential structure did not affect the results.

The currents of the emitter, extractor, and collector increased abruptly with the change in voltage polarity even without ionic liquid because they were located close to each other like capacitors. Therefore, we excluded the measurement data for the first 20 ms of the voltage alternation to eliminate the high-frequency components, and the measurement range of the current was set to 100 μA (accuracy of ±0.025 μA) in the experiments described below.

Figure 7 plots the onset voltage of ion emission as a function of the capillary inner diameter of the emitter. Ion emission was performed using the multiple emission areas integrated within the two wafers (Wafers A and B), as mentioned in Sect. 2.2. Here, the capillary diameter in Fig. 7 was taken from the averaged values of five emitters randomly

selected from each array. The ion emission started at 61 V using the emitter array with a 124-nm capillary diameter. The largest capillary diameter in this measurement was 261 nm, and the ion emission started at 71 V. It should be noted that only data at 261 nm were obtained from the emitter array fabricated on Wafer A, while the other data were obtained from Wafer B. The values of the onset voltages for capillary diameters of 157 nm, 209 nm, and 261 nm were measured twice using the same array. The solid line in Fig. 7 was obtained from the theoretical onset voltage under the assumption that the tip of the ionic liquid had a parabolic shape corresponding to

$$V_{\mathrm{s}} = \sqrt{\frac{\gamma r_{\mathrm{c}}}{\varepsilon_0}}\, ln \frac{2d}{r_{\mathrm{c}}}, \tag{4}$$

where r_{c} is the radius of curvature at the tip of the ionic liquid, γ is the surface tension (0.06127 N/m at 292.96 K for EMI-DCA),[29] ε_0 is the permittivity of free space, and d is the distance between the tip of the ionic liquid and the extractor, which was a flat plate (d = 1,000 nm).[30–32] The radius of curvature was assumed to be equal to the inner radius of the capillary emitter.[33] The values of the experimental data were smaller than the theoretical values, likely because the radius of curvature was overestimated and the extractor was not entirely flat. Nonetheless, they were qualitatively consistent with the theoretical estimation.

Figure 8 presents the current density as a function of the voltage applied to the extractor. The amplitude of the applied voltage was increased from 0 to 90 V by 1 V. The current was averaged for four measurement points for each voltage pulse. This result was obtained using 400 emitters arranged in a 20 × 20 array with 5-μm pitch from Wafer A, where the current

density was calculated with an emission area of 100 × 100 μm^2. The positive ion emission started at −72 V, and the positive current increased to 4.3 μA at −75 V. The negative ion emission also started at 72 V, and the negative current reached −1.3 μA at 77 V. Beyond 75 V of the absolute value of the extractor voltage, the extractor current increased due to the interception of emitted ions by the extractor, where the ions were emitted unstably, and leakage of ionic liquid occurred. Nonetheless, no extractor current was detected at voltages in the range of ±(72–75) V, indicating that ions were emitted stably without leakage of ionic liquid.

Regarding the current density, the maximum positive value was 43 mA cm^{-2}, while the negative value was −13 mA cm^{-2}. These current densities are approximately 50 and 9 times higher, respectively, than those of the previously fabricated emitter array on the positive and negative side,[13] and thus, more than 100 times higher than that of conventional electrospray thrusters on the positive side.[5] Assuming that an accelerator electrode is integrated into this array and the ions are accelerated by 1 kV acceleration voltage, the thrust density calculated from Eq. (1) can reach 2.1 mN cm^{-2} for positive ion emission and 0.48 mN cm^{-2} for negative ion emission. Here, the mass of EMI and DCA are 111 g mol^{-1} and 66 g mol^{-1}, respectively, and both positive and negative ions are assumed to be emitted as singly charged ions. In the case of positive ion emission, this estimation indicates that the thrust density is comparable to or higher than that of other plasma thrusters.[12]

Figure 9 illustrates the applied voltage of the bipolar pulse and currents of each electrode as a function of time. We used 400 emitters arranged in a 20 × 20 array with 5-μm

pitch from Wafer A. The amplitude of the applied voltage was increased from 0 to 72 V by 2 V at a repetition frequency of 5 Hz. After reaching the target voltage of ±72 V, the bipolar pulse voltage was continuously applied for approximately 20 s. The current was averaged for four measurement points for each voltage pulse. The collector current of the positive and negative ions started to increase at 11 s and 12 s, respectively, which indicated a delay of approximately 4 s from the time that the amplitude of the applied voltage became steady. This delay implies that the ionic liquid did not reach the emitter tip when the voltage was initially applied, and moved to the tip while the voltage was being applied. After the collector current of positive ions peaked to 1.4 μA at 12 s, the current decayed and converged to 300 nA. The collector current of negative ions was continuously in the range of 200–300 nA. It should be noted that a small extractor current was detected due to the current measurement accuracy (±0.025 μA). Therefore, the extractor current could be regarded as 0 during the measurement, indicating that the ionic liquid did not leak during operation.

4. Conclusions

In this paper, we fabricated a nano-capillary emitter array to increase the fluidic impedance for stable ion emission without leakage of ionic liquid. The nano-capillary emitter was successfully fabricated with a 100–300-nm capillary diameter that could be varied by adjusting the etch-back time. SiN was selected as the insulating material of the emitter to suppress the degradation of the emitter surface by electrochemical reactions. The SiN emitter was treated by CHF_3

plasma to prevent the ionic liquid from wetting and spreading.

After the fabrication, an ion emission experiment was conducted using EMI-DCA as a propellant. The starting voltage of ion emission was in qualitative agreement with the theoretical estimation. The maximum current density was 43 mA/cm^2 at a voltage of −75 V applied to the extractor and −13 mA/cm^2 at 77 V, which is 10–100 times higher than that of conventional electrospray thrusters. Assuming that an accelerator electrode is integrated into this array and the ions are accelerated by 1 kV acceleration voltage, the thrust density can reach 2.1 mN cm^{-2} for positive ion emission and 0.48 mN cm^{-2} for negative ion emission. For positive ion emission, this estimated thrust density is comparable to or higher than that of other plasma thrusters. Finally, we obtained continuous ion emission in a certain voltage range without current intercepted by the extractor, which indicates that ionic liquid did not leak during operation.

Acknowledgments

This work was supported in part by JSPS KAKENHI Grant Number JP18H01623, JAXA/RDD, and The Futaba Research Grant Program of the Futaba Foundation.

References

1) SpaceWorks Nano/Microsatellite Market Forecast 10th edition (2020).
2) S. Ciaralli, M.Coletti, and S.B.Gabriel, Acta Astronaut. **121**, 314 (2016).
3) S. J. Chung, S. Bandyopadhyay, R. Foust, G. P. Subramanian, and F. Y. Hadaegh, J. Spacecr. Rockets 53, 567 (2016).
4) H. Koizumi, K. Komurasaki, J. Aoyama, and K. Yamaguchi, Trans. Jpn. Soc. Aeronaut. Space. Sci., Aerosp. Technol. Jpn. **12**, Tb_19 (2014).
5) D. Krejci, F. Mier-Hicks, R. Thomas, T. Haag, and P. Lozano, J. Spacecr. Rockets **54**, 447 (2017).
6) K. Nakagawa, T. Tsuchiya, and Y. Takao, Jpn. J. Appl. Phys. **56**, 06GN18 (2017).
7) S. Dandavino, C. Ataman, C. N. Ryan, S. Chakraborty, D. Courtney, J. P. W. Stark, and H. Shea, J. Micromech. Microeng. **24**, 075011 (2014).
8) D. G. Courtney, S. Dandavino, and H. Shea, J. Propul. Power **32**, 392 (2016).
9) E. Grustan-Gutierrez and M. Gamero-Castaño, J. Propul. Power **33**, 984 (2017).
10) W. Deng, J. F. Klemic, X. Li, M. A. Reed, and A. Gomez, J. Aerosol Sci. **37**, 696 (2006).
11) Y. Kitazawa, K. Ueno, and M. Watanabe, Chem. Rec. **18**, 391 (2018).
12) K. Lemmer, Acta Astronaut. **134**, 231 (2017).
13) N. Inoue, M. Nagao, K. Murakami, S. Khumpuang, S. Hara, and Y. Takao, Jpn. J. Appl. Phys. **58**, SEEG04 (2019).
14) C. A. Spindt, I. Brodie, L. Humphrey, and E. R. Westerberg, J. Appl. Phys. **47**, 5248 (1976).
15) C. A. Spindt, Surf. Sci. **266**, 145 (1992).
16) J. Mach, T. Šamořil, S. Voborný, M. Kolíbal, J. Zlámal1, J. Spousta, L. Dittrichová, and T. Šikola, Rev. Sci. Instrum. **82**, 083302 (2011).
17) D. M. Goebel and I. Katz, *Fundamentals of Electric Propulsion; Ion and Hall Thrusters* (Wiley, Hoboken, NJ, 2008).
18) P. Lozano and M. Sanchez, J. Colloid Interface Sci. **280**, 149 (2004).
19) N. Brikner and P. Lozano, Appl. Phys. Lett. **101**, 193504 (2012).
20) R. Krpoun, K. L. Smith, J. P. W. Stark, and H. R. Shea, Appl. Phys. Lett. **94**, 163502 (2009).

21) C. Guerra-Garcia, D. Krejci, and P. Lozano, J. Phys. D Appl. Phys. **49**, 115503 (2016).

22) M. Nagao, T. Matsukawa, S.Kanemaru, J. Itoh, and H. Tanabe, J. Vac. Sci. Technol. B **19**, 920 (2001).

23) R. Cook, J. A. Nabity, and J. W. Daily, J. Propul. Power **33**, 1325 (2017).

24) M. Nagao and T. Yoshida, Microelectron Eng. **132**, 14 (2015).

25) M. Nagao, Y. Gotoh, Y. Neo, and H. Mimura, J. Vac. Sci. Technol. B **34**, 02G108 (2016).

26) T. Soda, M. Nagao, C. Yasumuro, S. Kanemaru, T. Sakai, N. Saito, Y. Neo, T. Aoki, and H. Mimura, Jpn. J. Appl. Phys. **47**, 5252 (2008).

27) S. Khumpuang and S. Hara, IEEE Trans. Semicond. Manuf. **28**, 393 (2015).

28) S. Khumpuang, F. Imura, and S. Hara, IEEE Trans. Semicond. Manuf. 28, 551 (2015).

29) J. Klomfar, M. Souckova, and J. Patek, J. Chem. Eng. Data **56**, 3454 (2011).

30) P. D. Prewett and G. L. R. Mair, *Focused Ion Beams from Liquid Metal Ion Sources* (Wiley, Hoboken, NJ, 1991).

31) P. Lozano and M. Sanchez, J. Colloid Interface Sci. **282**, 415 (2005).

32) A. Kimber, B. Jorns, and H. Sodano, 2018 Joint Propulsion Conference, AIAA 2018-4653.

33) R. Krpoun and H. R. Shea, J. Appl. Phys. 104, 064511 (2008).

List of Figure Captions

Fig. 1. Schematic of an internally fed electrospray thruster. A high-voltage bipolar pulse is applied between the emitter and extractor electrode.

Fig. 2. (a) Cross-sectional and (b) top views of a high-density emitter array together with extractor and accelerator electrodes. Nano-capillary emitters with 5-μm pitch are fabricated within several 100 μm diameters of the ionic liquid reservoir. The extractor aperture is aligned with each emitter to extract ions while the accelerator aperture is of the same order as the reservoir diameter to accelerate the extracted ions. Note that the voltage is not directly applied to the emitter but to the distal electrode.

Fig. 3. Contact angles of EMI-DCA on (a) SiN film treated by CHF_3 plasma and (b) untreated SiN, where 1.5 μL of EMI-DCA was dropped on each material. These contact angles were calculated by the half-angle method.

Fig. 4. Fabrication procedure of the nano-capillary emitter array. (a) First, a thin Al layer was deposited on the Si wafer, and Spindt-type Ni emitters were formed on it. (b) After the deposition of a thin SiN layer over the emitters, the SiN layer at the tip of the emitters was etched using the etch-back technique. (c) SiO_2 and Nb were deposited in series. The extractor

aperture was also formed similarly by the etch-back technique. (d) Removing SiO_2 by the BHF wet etching process opened the emitter tip. (e) After protecting the outside of the emitter array by photoresist and forming the Cr mask on the back side of the wafer, the deep-RIE process was performed. (f) Finally, the Al layer and the Ni emitters were removed.

Fig. 5. SEM images of (a) the 5-μm pitch nano-capillary emitter array and (b) one set of an emitter and extractor. The inset in (b) presents the top view of the emitter.

Fig. 6. Schematic of the experimental setup for measurement of the ion emission current.

Fig. 7. Onset voltage of ion emission (open squares) versus capillary diameter. The solid line follows the theoretical onset voltage expressed as a function of the curvature radius at the tip of the ionic liquid (see Eq. (4)), which is assumed to be equal to the capillary radius here.

Fig. 8. Current and the current density of the emitter (open circles), extractor (open squares), and collector (open triangles) as a function of the voltage applied to the extractor.

Fig. 9. (a) Applied extractor voltage, (b) collector currents of positive ions (open circles) and negative ions (open triangles), and extractor current (open squares) as a function of time.

360 **Fig. 1**

361

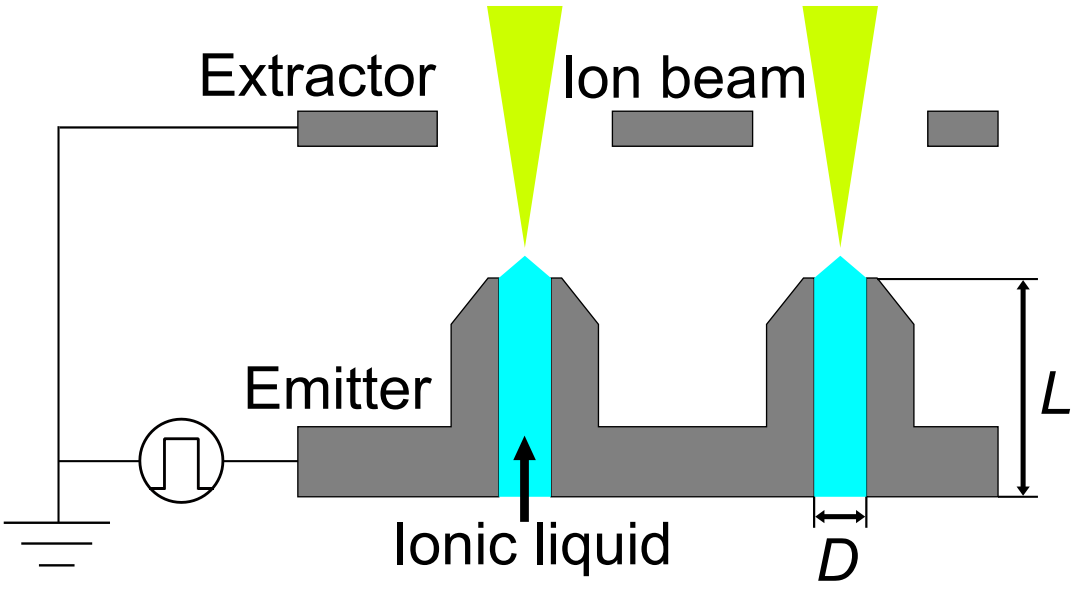

362 **Fig. 2**

363

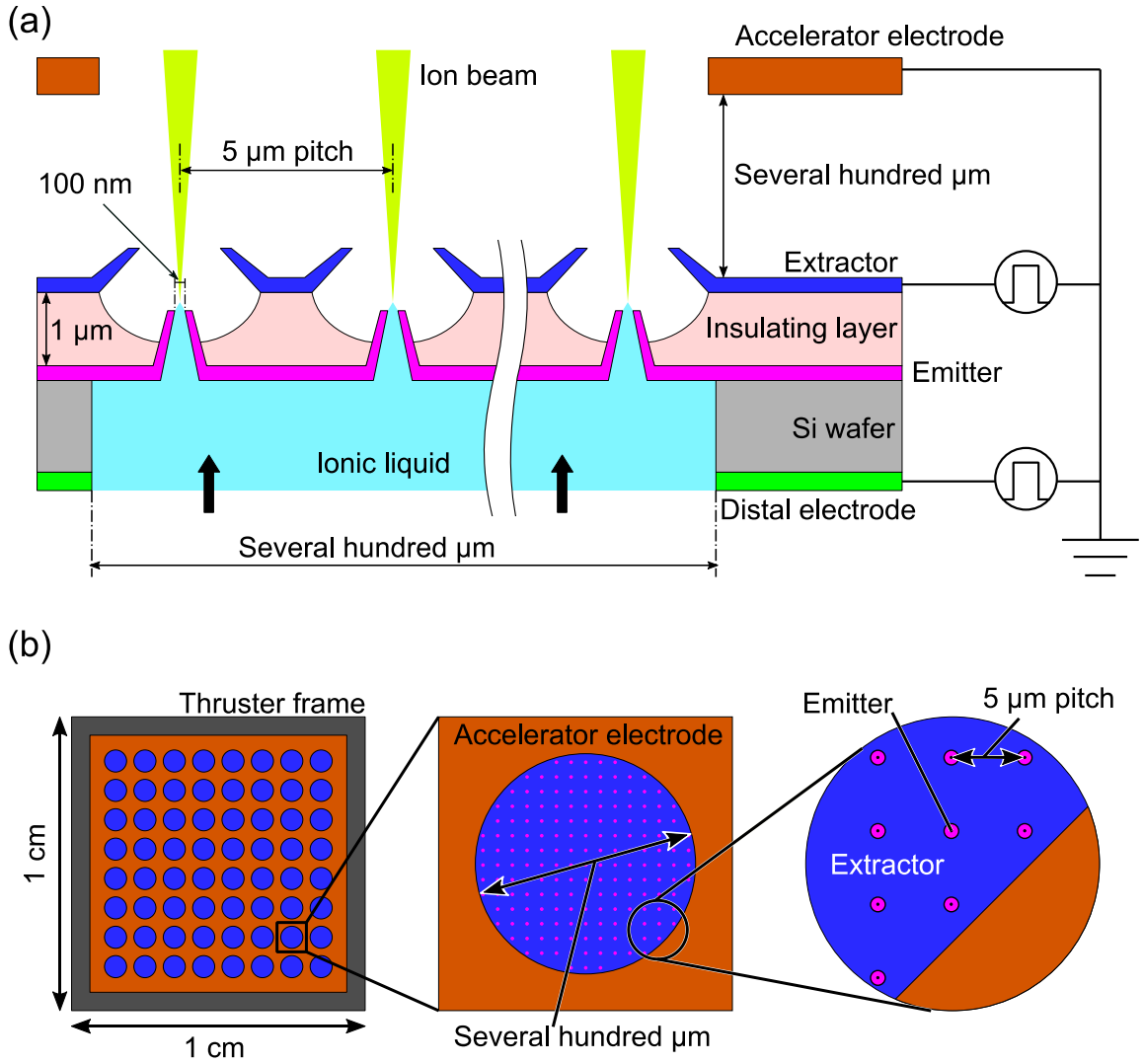
(a)
Accelerator electrode
Ion beam
5 μm pitch
100 nm
Several hundred μm
Extractor
1 μm
Insulating layer
Emitter
Si wafer
Ionic liquid
Distal electrode
Several hundred μm
(b)
Thruster frame
Accelerator electrode
Emitter
5 μm pitch
Extractor
1 cm
1 cm
Several hundred μm

364 **Fig. 3**

365

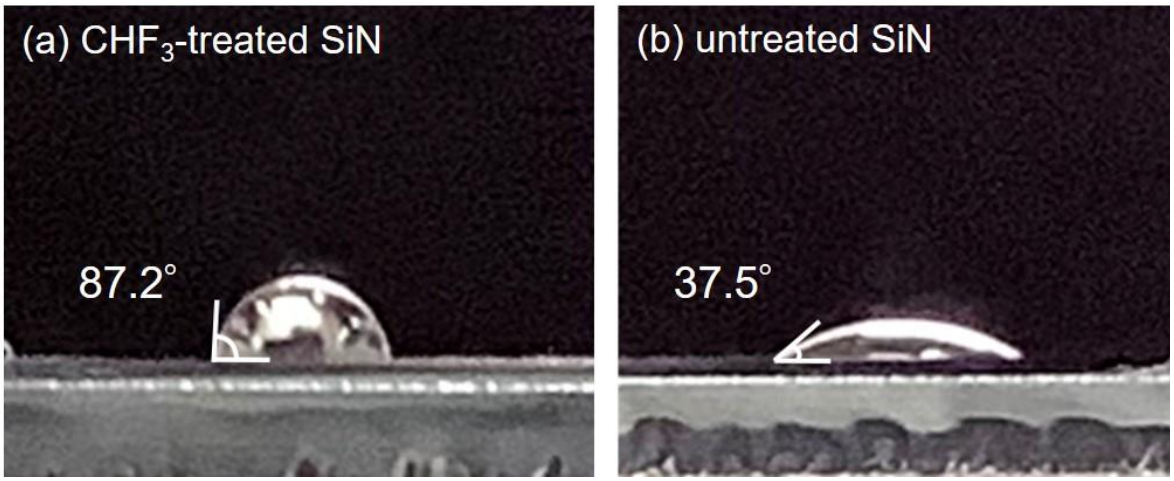

366 **Fig. 4**

367

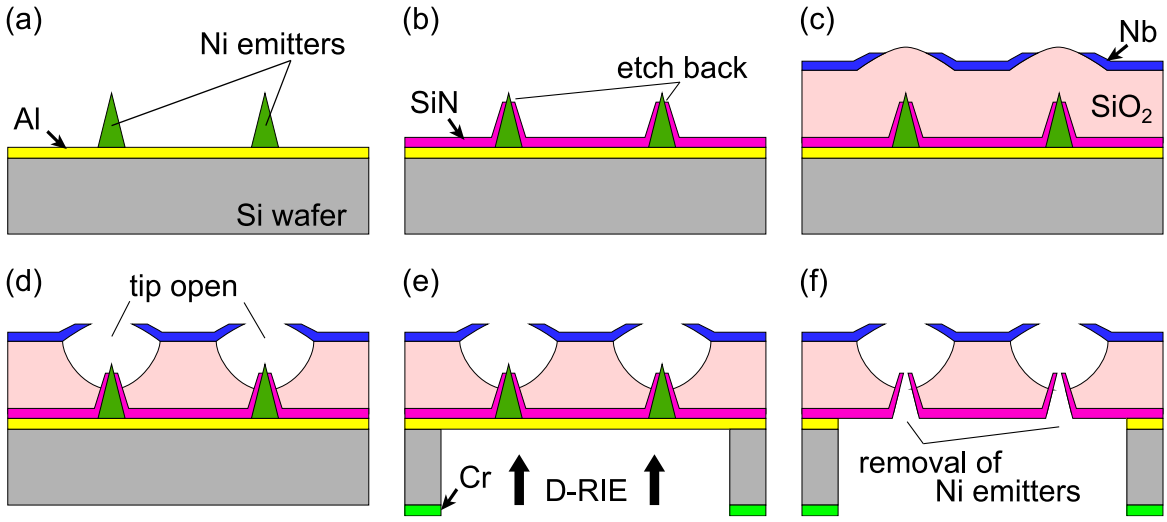
(a)
Ni emitters
Al
Si wafer
(b)
etch back
SiN
(c)
Nb
SiO_2
(d)
tip open
(e)
Cr
D-RIE
(f)
removal of
Ni emitters

368 **Fig. 5**

369

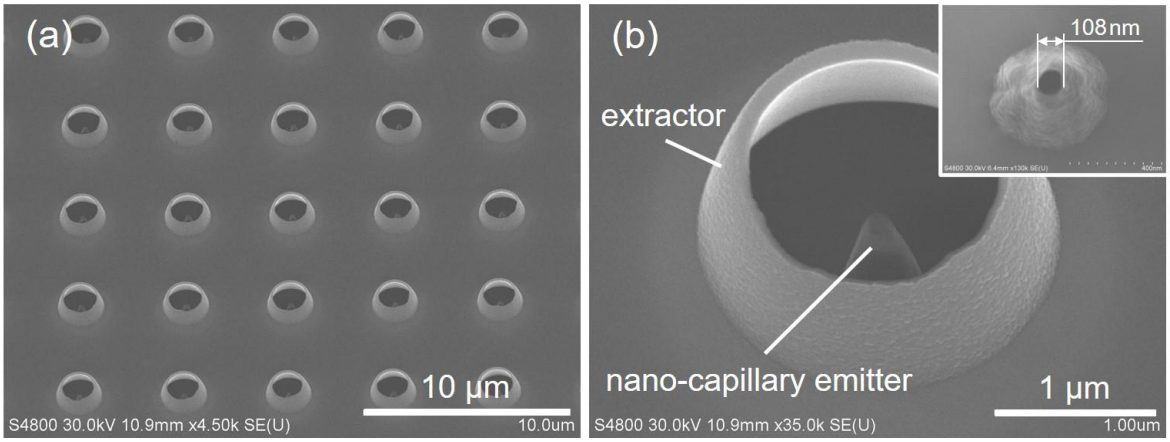
(a)
10 μm
S4800 30.0kV 10.9mm x4.50k SE(U)
10.0um
(b)
extractor
nano-capillary emitter
108nm
1 μm
S4800 30.0kV 10.9mm x35.0k SE(U)
1.00um

370 **Fig. 6**

371

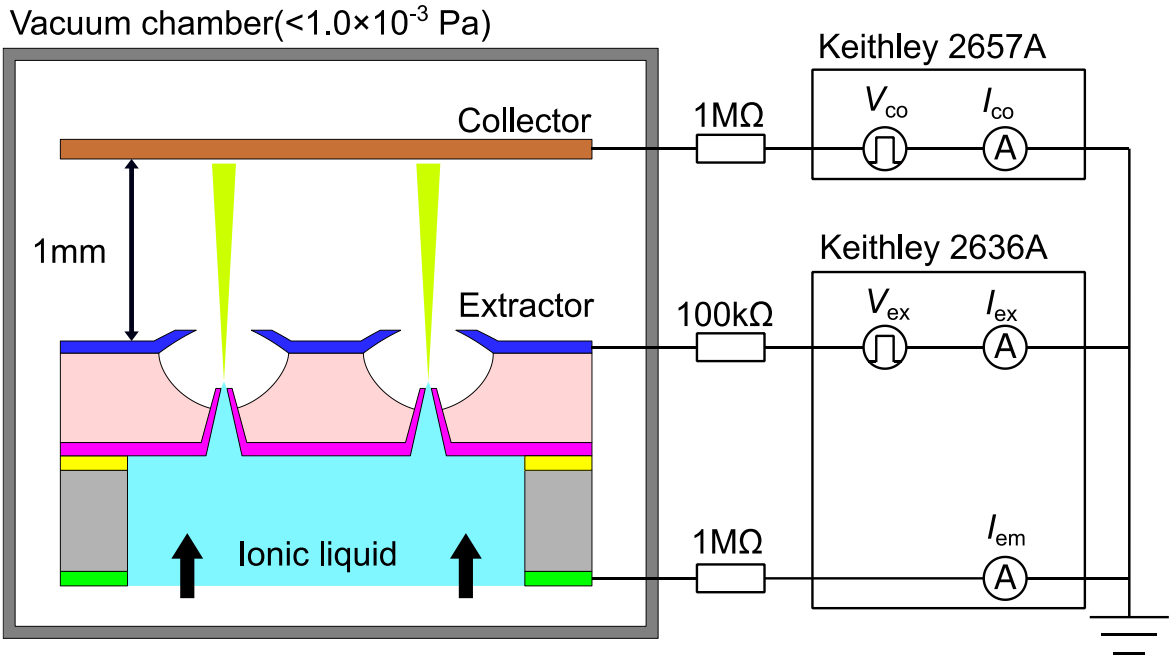
Vacuum chamber(<1.0×10-3 Pa)
Collector
1mm
Extractor
Ionic liquid
1MΩ
100kΩ
1MΩ
Keithley 2657A
Vco
Ico
A
Keithley 2636A
Vex
Iex
A
Iem
A

372 **Fig. 7**

373

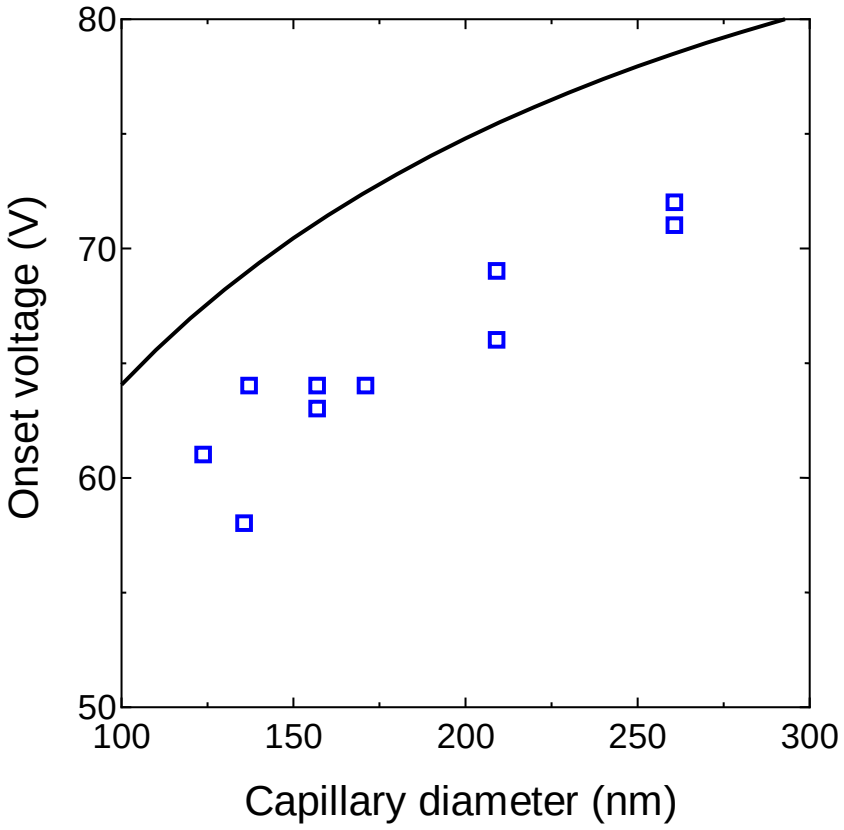
80
70
60
50
100
150
200
250
300
Onset voltage (V)
Capillary diameter (nm)

374 **Fig. 8**

375

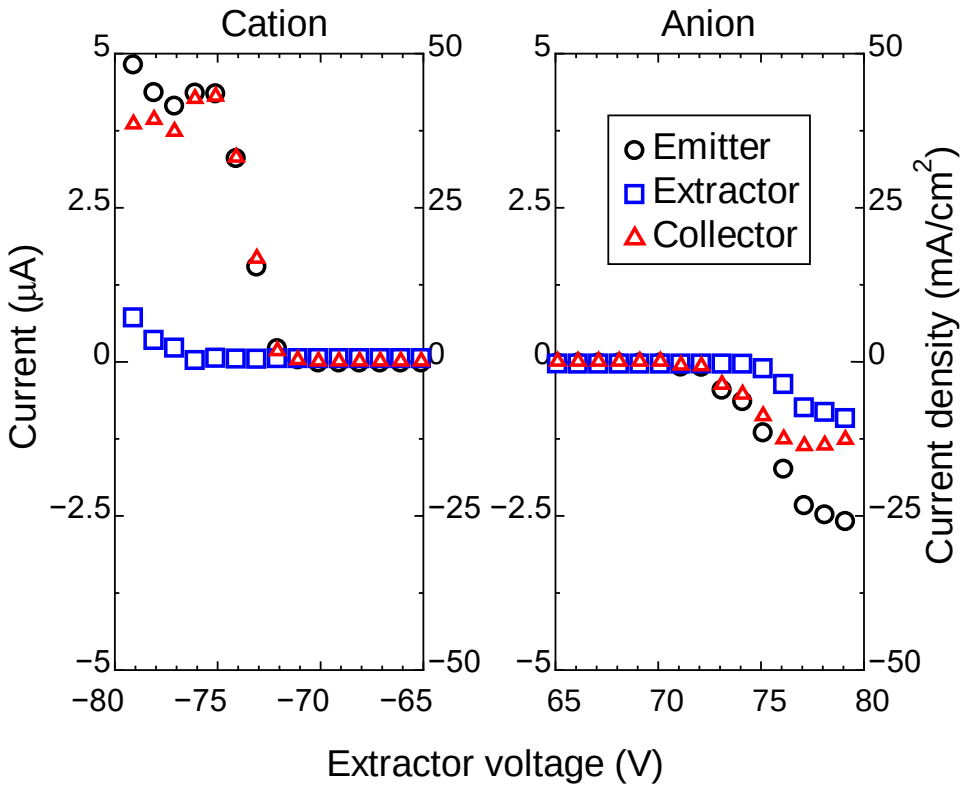
Cation
Anion
Emitter
Extractor
Collector
Current (μA)
Current density (mA/cm^2)
Extractor voltage (V)
5
2.5
0
−2.5
−5
50
25
0
−25
−50
−80
−75
−70
−65
65
70
75
80

376 **Fig. 9**

377

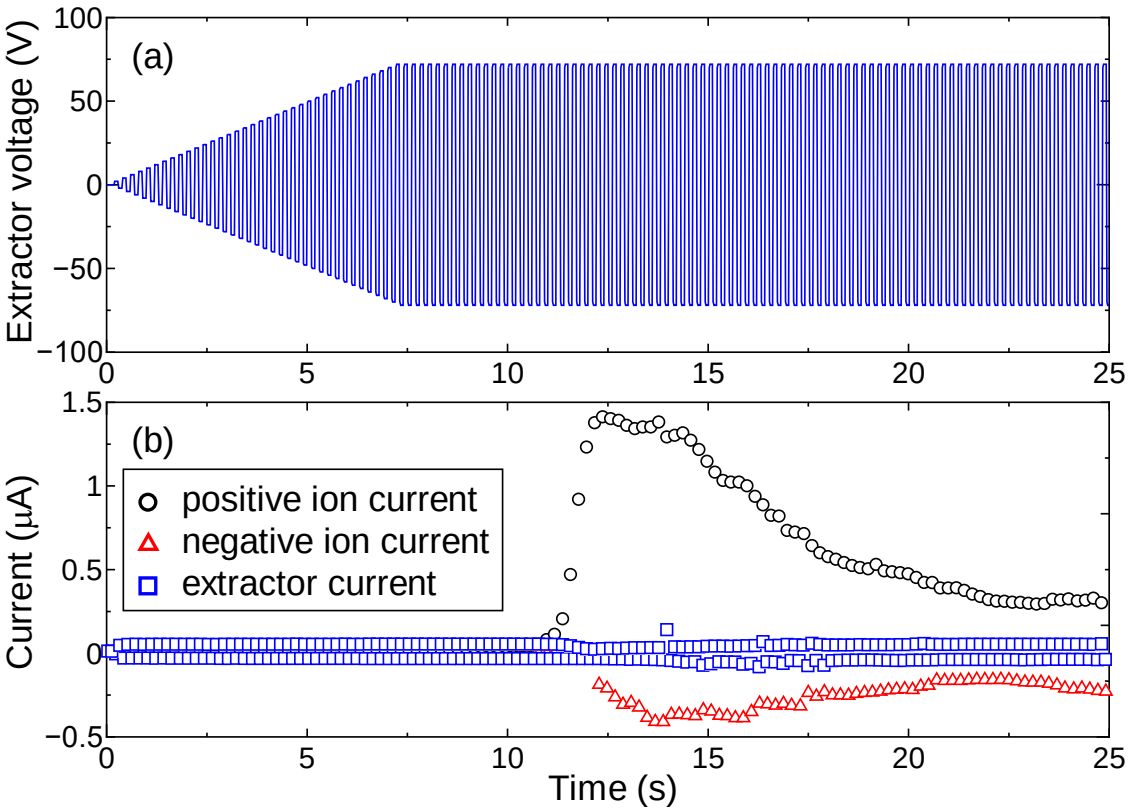
(a)
Extractor voltage (V)
100
50
0
−50
−100
0
5
10
15
20
25
(b)
positive ion current
negative ion current
extractor current
Current (μA)
1.5
1
0.5
0
−0.5
Time (s)